CHEMISTRY
AN ASIAN JOURNAL

DOI: 10.1002/asia.201200578

Reaction-Based Colorimetric and Ratiometric Fluorescence Sensor for Detection of Cyanide in Aqueous Media

Yan-Duo Lin,[a] Yung-Shu Pen,[b] Weiting Su,[c] Kang-Ling Liau,[d] Yun-Sheng Wen,[a] Chin-Hsin Tu,[b] Chia-Hsing Sun,[b] and Tahsin J. Chow*[a]

Abstract: A stilbene-based compound (**1**) has been prepared and was highly selective for the detection of cyanide anion in aqueous media even in the presence of other anions, such as F^-, Cl^-, Br^-, I^-, ClO_4^-, $H_2PO_4^-$, HSO_4^-, NO_3^-, and $CH_3CO_2^-$. A noticeable change in the color of the solution, along with a prominent fluorescence enhancement, was observed upon the addition of cyanide. The color change was observed upon the nucleophilic addition of the cyanide anion to the electron-deficient cyanoacrylate group of **1**. The spectral changes induced by the reaction were analyzed by comparison with two model compounds, such as compound **2** with dimethyl substituents and compound **3** without a cyanoacrylate group. An intramolecular charge-transfer (ICT) mechanism played a key role in the sensing properties, and the mechanism was supported by DFT/TDDFT calculations.

Keywords: anions · chemodosimeter · cyanides · fluorescence · sensors

Introduction

Anions play important roles in the chemistry of biology, medicine, and catalysis.[1] Among them, the cyanide ion is unique owing to its lethal effect on living organisms and the influence it has on our environment.[2] Nevertheless, cyanide is widespread in industrial processes, including gold mining, electroplating, metallurgy, and the synthesis of fibers and resins.[3] The accidental or intentional release of toxic chemicals can contaminate drinking water and become a serious threat to the environment. Therefore, the detection of cyanide has become a subject of much attention in recent years. Versatile methods for the detection of cyanide have been developed, such as those based on hydrogen-bonding interactions, complex formations with metal ions and boron derivatives, and the attachment with quantum dots, etc.[4,5] Reaction-based chemosensors for cyanide anion were also used by taking advantage of their high selectivity over other anions, especially in aqueous solutions. This chemosensor can effectively reduce the interference of hydrogen bonding and the acidity of the media. Effective sensors have been designed using squaraine,[6] acridium salts,[7] oxazines,[8] trifluoroacetophenone derivatives,[9] benzyl derivatives,[10] and dicyanovinyl derivatives.[11]

Among the various signals for detection, fluorescence emission is regarded to be the most efficient owing to its high sensitivity and easy implementation under diversified environmental conditions.[12] Usually, fluorescence detection depends on the intensity change at a single wavelength. The signal output could be easily overshadowed by the background noise of the sample media. To overcome this shortcoming, ratiometric fluorescent sensing is used, and this allows the measurement of relative fluorescence intensities at two different wavelengths.[13] The proportional ratio between the two different emissions can serve as an internal reference for self-correction, therefore the reliability of the measurements is substantially enhanced.[12b,14] To date, only limited examples of ratiometric fluorescent chemosensors of cyanide have been reported.[15]

To design a ratiometric probe that functions at two different wavelengths, either a fluorescence resonance energy transfer (FRET) or an intramolecular charge transfer (ICT) mechanism can be adopted.[15] Herein we report a high-performance colorimetric and ratiometric fluorescent chemosensor (**1**) for cyanide that is based on the ICT mechanism. This sensor works effectively in aqueous media with a distinctive visual color change and a large signal amplification (2250 fold) upon fluorescence; uses an electron-rich *trans*-4-(*N*,*N*-diphenylamino)stilbene (**3**) as a fluorescence emitter[16]

[a] Dr. Y.-D. Lin, Y.-S. Wen, Prof. Dr. T. J. Chow
Institute of Chemistry
Academia Sinica
Taipei 115 (Taiwan)
Fax: (+886) 2-27884179
E-mail: chowtj@gate.sinica.edu.tw

[b] Dr. Y.-S. Pen, C.-H. Tu, Prof. Dr. C.-H. Sun
Department of Chemistry
Soochow University
Taipei 111 (Taiwan)

[c] W. Su
Department of Chemistry
National Taiwan University
Taipei 106 (Taiwan)

[d] Dr. K.-L. Liau
Department of Chemistry
National Central University
Chung-Li 320 (Taiwan)

Supporting information for this article is available on the WWW under http://dx.doi.org/10.1002/asia.201200578.

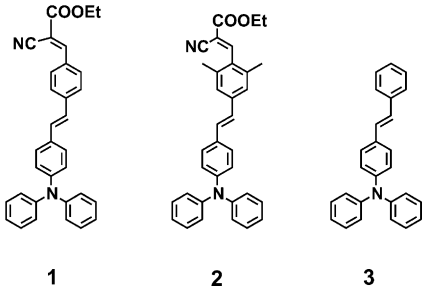

and a 2-cyanoacrylate as a detecting unit (Scheme 1). Upon photoexcitation, compound **1** displays a strong ICT absorption. However, the fluorescence quantum yield is relatively

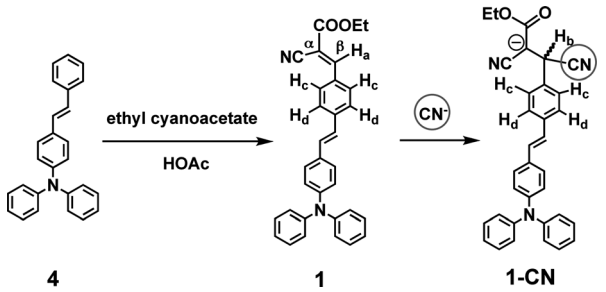

Scheme 1. Synthesis of compound **1** and the reaction of **1** with the cyanide anion for the formation of **1-CN**.

low owing to polarity quenching of the charge-separated state. The sensing mechanism is recognized by a nucleophilic addition of cyanide to the β-position of 2-cyanoacrylate.[11e] The interruption in the π-conjugation between the stilbene and the carboxylate, therefore terminates the ICT. As a consequence, the color of the solution fades (blue shift in the UV region), and at the same time a strong π–π* fluorescence from the stilbene chromophore emerges. The detection of the cyanide ion can be clearly observed by a discernible color change in both the absorption and emission spectra.

Results and DiscussionSynthesis and Crystal Structure

The synthesis of compounds **1** and **2** are outlined in Schemes 1 and 2. The synthesis of **3**,[16a] **4**,[17] **5**,[18] and **6**[17] have been previously reported. The synthesis of **1** was achieved readily through condensation of aldehyde **4**[17] with ethyl cyanoacetate in the presence of acetic acid. Compound **6**[17] was coupled with 4-bromo-2,6-dimethyl-benzaldehyde through a Heck-type reaction to afford **7**, followed by a Knoevenagel reaction with ethyl cyanoacetate to afford the desired compound **2**.

A single crystal of compound **1** was resolved by X-ray diffraction analyses, and its molecular structure is shown in Figure 1.[19] From the side view it is clearly observed that the 2-cyanoacrylic acid ethyl ester group is coplanar with the

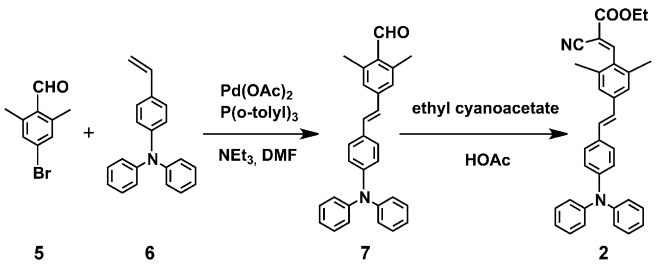

Scheme 2. Synthesis of compound **2**.

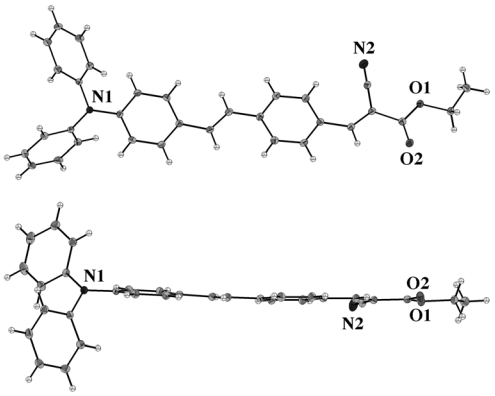

Figure 1. The X-ray crystal structures of **1** with displacement atomic ellipsoids drawn at the 30% probability level.

stilbene moiety. Such planar conformation provides efficient π-conjugation and favors the efficient ICT transition between the donor and the acceptor groups. Another structural feature worth noting is the planar conformation of the substituents around the nitrogen atom. The sum of the bond angles (θ) around the nitrogen atom is about 355°, thereby indicating that the three phenyl substituents are in an ideal trigonal planar arrangement. This ensures an effective delocalization of the amine lone pair to the adjacent π-systems.[20] A strong dipole is therefore expected in the ICT state upon photoexcitation.

Colorimetric and Absorption Spectral Response

The photophysical properties of the compounds **1**–**3** and **1-CN** in water/tetrahydrofuran (THF) solutions are summarized in Table 1. The sensing properties of **1** were examined in water/THF solutions (30:70 (v/v)) by the addition of the tetrabutylammonium (TBA) salt of various anions such as F^-, Cl^-, Br^-, I^-, ClO_4^-, $H_2PO_4^-$, HSO_4^-, NO_3^-, $CH_3CO_2^-$, and with and without CN^- (Figure 2a). In the UV/Vis absorption spectrum, the solution of **1** showed two distinct absorption bands at 310 and 446 nm. The former is attributed to the π–π* transition and the latter to an ICT transition. Upon addition of 30 equivalents of various anions except for CN^- ion, the absorption spectra of sensor **1** did not exhibit any significant change. However, upon addition of CN^- ion, both absorption bands diminished with concomi-

CHEMISTRY
AN ASIAN JOURNAL

Table 1. Maxima of UV/Vis absorption (λ_{abs}), fluorescence (λ_f), fluorescence decay times (τ_{fl}), 0,0 transition ($\lambda_{0,0}$), and fluorescence quantum yields (Φ_{fl}) for compounds **1**–**3** and **1-CN** in water/THF solutions.

Compound	λ_{abs} [nm]	λ_f [nm]	λ_{0-0} [nm][a]	τ_{fl}	Φ_{fl}
1	310, 446	460, 676	533	2.48[b]	0.012
1-CN	296, 373	460	419	n.d[c]	0.66
2	305, 394	500, 655	474	2.90[b]	0.031
3	296, 366	455	405	2.41[d]	0.89

[a] The value of λ_{0-0} was obtained from the intersection of normalized absorption and fluorescence spectra. [b] The value of τ_{fl} was determined with excitation around the spectral maxima and emission around 460 nm for **1** and 500 nm for **2**. [c] Not determined. [d] The value of τ_{fl} was determined with excitation and emission around the spectral maxima.

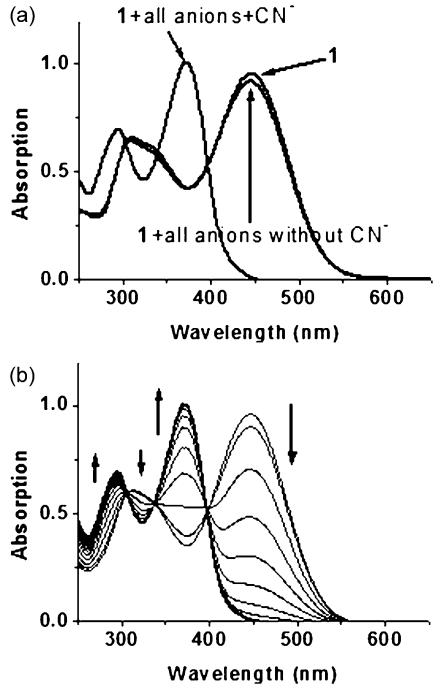

Figure 2. a) Absorption spectra of **1** in a water/THF (30:70, v/v) solution (3×10^{-5} M), and F^-, Cl^-, Br^-, I^-, ClO_4^-, $H_2PO_4^-$, HSO_4^-, NO_3^-, $CH_3CO_2^-$ with and without CN^- (30 equiv each); b) Absorption titration spectra of **1** with different concentrations of CN^- ($0\approx30$ equiv at 2.0 equiv intervals).

tant growth of two new bands at 296 and 373 nm (Figure 2b). The time-dependence changes in the absorption spectra of sensor **1** upon the addition of cyanide were almost completed within 14 min, as indicated in Figure 3. The presence of three clear isosbestic points at 305, 338, and 397 nm implies its clean transformation into a new species (Figure 2b). This is in good agreement with a 1:1 binding stoichiometry by Job's plot of the UV/Vis absorption (Figure 4). The significant changes in the color can be perceived clearly by the naked eye (Figure 5). The color change is attributed to the nucleophilic addition of CN^- to the β-position of 2-cyanoacrylic acid ethyl ester, thereby leading to a significant blue shift in the absorption wavelength (Scheme 1). The spectral response is predictable in neutral and basic solutions, yet in an acidic solution ($pH\leq5$), the detecting sensitivity is substantially reduced due to the pro-

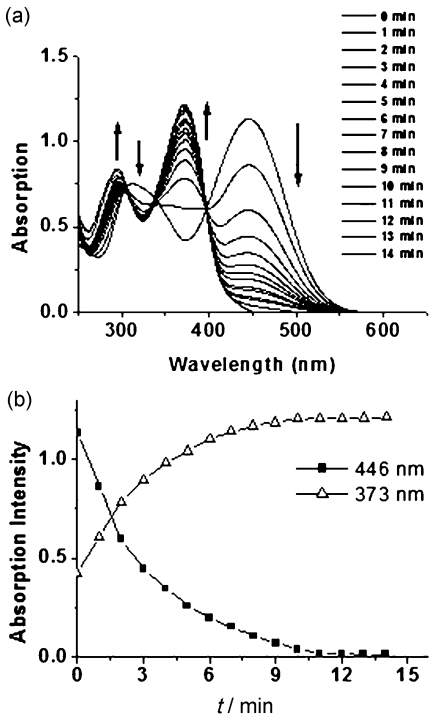

Figure 3. a) Time-dependent absorption spectra of sensor **1** (3×10^{-5} M) upon the addition of CN^- (10 equiv) in a water/THF (30:70, v/v) solution. The arrows indicate the change in incubation time from 0 to 14 mins. b) Time-dependent absorption intensity of sensor **1** at 446 nm (■) and 373 nm (△) in the presence of CN^- (10 equiv).

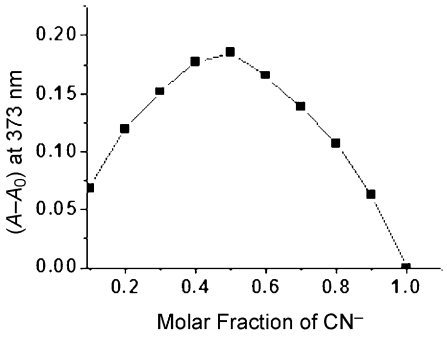

Figure 4. Job's plot of **1** in a water/THF (30:70, v/v) solution showing the 1:1 stoichiometry of the reaction with CN^-. The total concentration of **1** and CN^- is 10^{-5} mol L^{-1}. Absorbance is recorded at 373 nm.

tonation of CN^- (Figure S11, see the Supporting Information).

Fluorescence Behavior

When compound **1** was photoexcited, a weak red fluorescence centered at 676 nm was observed ($\Phi_f=0.012$, excited at the isosbestic point 338 nm). Along with this major emission band, a minor emission band centered at 460 nm can also be observed (Figure 6a). The ICT nature of compound **1** at the 676 nm band is unambiguously supported by the solvent-polarity dependent spectral shift, as depicted in Fig-

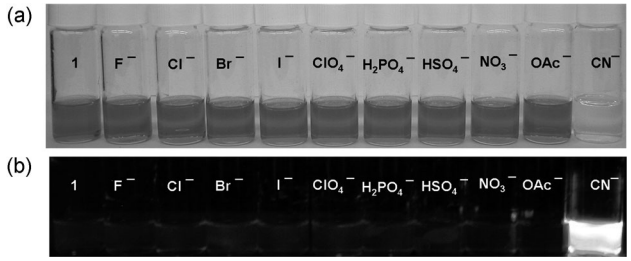

Figure 5. a) Color changes of **1** (3×10^{-5} M) after addition of F^-, Cl^-, Br^-, I^-, ClO_4^-, $H_2PO_4^-$, HSO_4^-, NO_3^-, $CH_3CO_2^-$, and CN^- (30 equiv, respectively) in water/THF (30:70, v/v); b) fluorescence change of **1** (3×10^{-5} M) after addition of F^-, Cl^-, Br^-, I^-, ClO_4^-, $H_2PO_4^-$, HSO_4^-, NO_3^-, $CH_3CO_2^-$ and CN^- (30 equiv, respectively) in water/THF (30:70, v/v) upon excitation at 365 nm with a laboratory UV lamp.

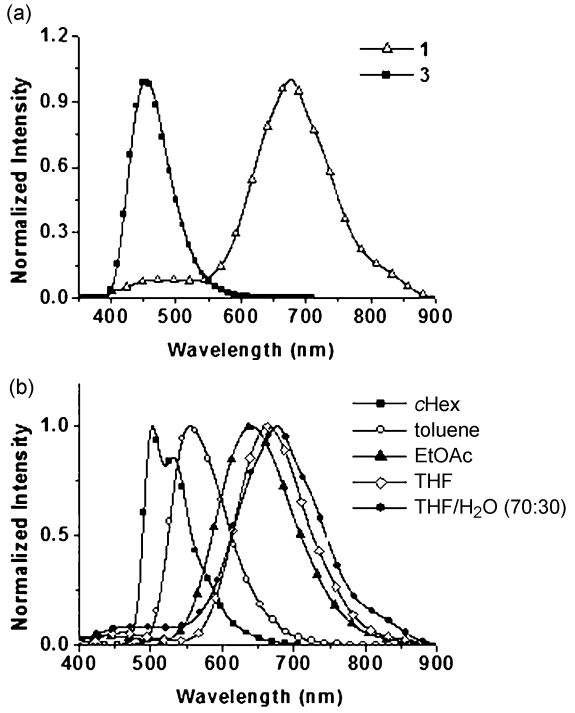

Figure 6. a) Normalized fluorescence spectra of **1** and **3** in a water/THF (30:70, v/v) solution; b) Normalized fluorescence spectra of sensor **1** in cyclohexane, toluene, ethyl acetate, THF, and water/THF (30:70, v/v).

ure 6b. The emission band at 460 nm is most likely derived from the *trans*-4-(*N*,*N*-diphenylamino) stilbene moiety (c.f., compound **3** at λ_{max} 455 nm Figure 6a), as the result of an out-of-plane twist between the stilbene and 2-cyanoacrylate moieties. The excitation spectra were also obtained by monitoring the emission at 460 nm, and the excitation spectra of **1** was in good agreement with the absorption spectra of **3**, thereby suggesting that the emission of **1** at 460 nm is derived from a similar chromophore to that of **3** (Figure S7a, see the Supporting Information). The fluorescence lifetime (τ_f) of **1** at 460 nm ($\tau_f=2.48$ ns) is also close to that of **3** at 455 nm ($\tau_f=2.90$ ns). To shed more light on the origin of the dual fluorescence, a dimethyl-substituted derivative **2** was synthesized for comparison. In a simulated structure of compound **2**, by using DFT calculations (Figure S8, see the Supporting Information), the dihedral angle between the 2-cyanoacrylate and the adjacent phenyl group was twisted to approximately 50° in its lowest energy state. The presence of dual fluorescence of **2** at 500 and 655 nm in aqueous solution resembles closely to that of **1** (Figure 7). The intensity of the 500 nm emission of **2** was found to be higher than the

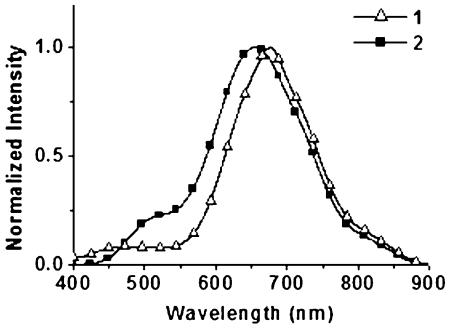

Figure 7. Normalized fluorescence spectra of **1** and **2** in a water/THF (30:70, v/v) solution.

460 nm emission of **1**, as a result of a higher population of the twist conformation. The excitation spectrum of **2** coincides with the absorption maximum of **3** (Figure S7b, see the Supporting Information). The lifetime of the 500 nm emission ($\tau_f=2.41$ ns) of **2** was also quite close to that of **1** at 460 nm. All of this information supports the conclusion that the minor emission band of **1** is derived from a twisted conformational isomer, which forms an equilibrium with the major planar conformational isomer.[15f,21]

Anions-Induced Fluorescence Spectral Response

Upon the addition of F^-, Cl^-, Br^-, I^-, ClO_4^-, $H_2PO_4^-$, HSO_4^-, NO_3^-, and $CH_3CO_2^-$, no significant change was observed in the emission spectra of **1**. The only prominent response appeared when CN^- was added (Figure 8a), while fluorescence was observed at 460 nm and the band at 676 nm diminished. The blue shift induced by the addition of CN^- was very large (216 nm) with a clear isoemissive point at 643 nm. The intensive blue fluorescence can be easily observed by the naked eye (Figure 5b). The ratio of fluorescence intensities at 460 nm and 676 nm (I_{460}/I_{673}) exhibited a 2.25×10^3 fold in enhancement, that is, from 0.08 to 180 ($\Phi_f=0.66$) before and after the addition of CN^- (30 equiv), respectively. To further elucidate the effectiveness of sensor **1** under harsher conditions, a competitive experiment was examined in a water/THF solution in the presence of the following anions: F^-, Cl^-, Br^-, I^-, ClO_4^-, $H_2PO_4^-$, HSO_4^-, NO_3^-, and $CH_3CO_2^-$ (30 equiv each). The color of the solution changed from orange to colorless upon the addition of CN^- in the same manner as those by adding each anion alone (Figure 2a). The strong fluorescence enhancement was not affected either by the presence of all

CHEMISTRY
AN ASIAN JOURNAL

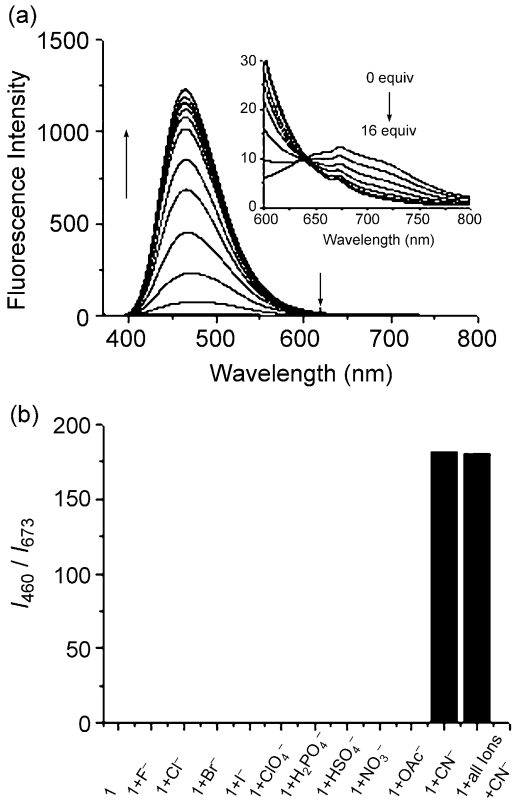

Figure 8. a) Fluorescence titration spectra of **1** (3×10^{-5} M in water/THF 30:70, v/v) in solution with different concentrations of CN^- ($0\approx30$ equiv at 2.0 equiv interval). Inset: ratio of fluorescent intensities at 676 and 460 nm as a function of CN^- concentration; b) The fluorescence ratio intensity of **1** (3×10^{-5} M) at 460 nm and 673 nm in the presence of various analytes (30 equiv) in a water/THF (30:70, v/v) solution.

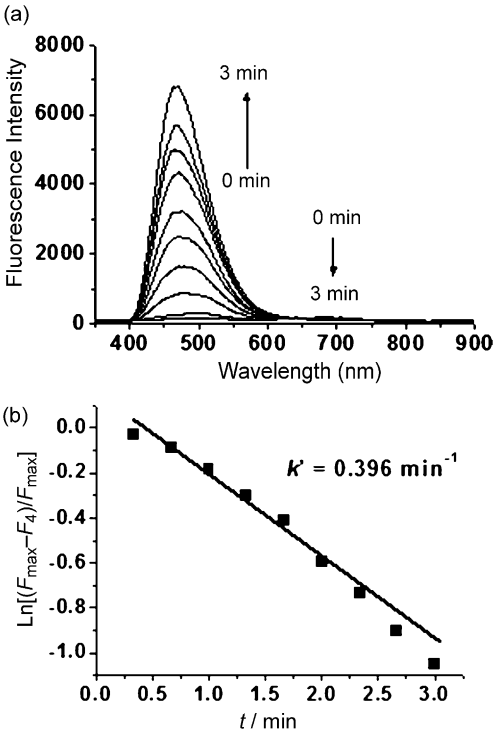

Figure 9. a) The fluorescence intensity of sensor **1** (3×10^{-5} M) incubated with CN^- (6×10^{-4} M) for 0–3 min. b) *Pseudo*-first-order kinetic plot of the reaction of **1** (3×10^{-5} M) incubated with CN^- (6×10^{-4} M) in a water/THF (30:70, v/v) solution. Slope $=-0.396$ min^{-1}.

anions together (Figure 8b). These experiments not only confirmed the excellent selectivity of **1** for the cyanide anion, but also illustrated its high potential for practical applications.

Kinetic Studies

The reaction rate constant of **1** (3×10^{-5} M) with CN^- (6×10^{-4} M) was estimated under a *pseudo*-first-order approximation (Figure 9). The reaction of sensor **1** (3×10^{-5} M) with CN^- (6×10^{-4} M) in a water/THF (30:70, v/v) solution was monitored by using the fluorescence intensity at 460 nm (Figure 9a). The reaction was carried out at room temperature. The *pseudo*-first-order rate constant for the reaction was determined by fitting the fluorescence intensities of the samples to the *pseudo*-first-order equation (1):

$$\ln\left[(F_{max}-F_t)/F_{max}\right] = -k't \quad (1)$$

where F_t and F_{max} are the fluorescence intensities at 460 nm at time t and the maximum value obtained after the reaction was completed. k' is the *pseudo*-first-order rate constant. The *pseudo*-first-order plot for the reaction of **1** with CN^- (6×10^{-4} M) is shown in Figure 9b. The negative slope of the line provides the *pseudo*-first-order rate constant for CN^-: $k'=0.396$ min^{-1}.

^{1}H NMR Titration Experiments

The product **1-CN** was analyzed by ^{1}H NMR spectroscopy. A solution of **1** in [D_8]THF solution was monitored by gradual addition of tetrabutylammonium cyanide (Figure 10). The increase in cyanide concentration resulted in a diminished vinylic proton signal (H_a) at 8.24 ppm, until it completely disappeared with the addition of 1 equiv of cyanide anion. A new signal appeared at 5.04 ppm, which corresponds to the β-proton of cyanoacrylate. Meanwhile, the two sets of aromatic protons (H_c and H_d in the styrene moiety) are shifted to higher field with respect to the ethylene protons. These observations are consistent with the pro-

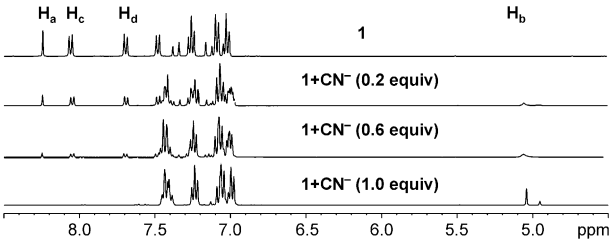

Figure 10. ^{1}H NMR spectral changes of **1** in [D_8]THF upon the addition of CN^- anion.

posed mechanism shown in Scheme 1. However, no signal was observed that corresponds to the α-proton of the ethylene moiety due to the persistence of a stabilized enolate anion.[4d] In addition, the formation of cyanide adduct **1-CN-H** (i.e., neutral form of anion **1-CN**) was further confirmed by high-resolution FAB-MS, where a peak at m/z 498.2190 is assigned to $[\mathbf{1\text{-}CN} + 2H]^+$ (Figure S9, see the Supporting Information).

Molecular Orbital Calculations

To gain further insight into the mechanism of the color bleaching and fluorescence enhancement of **1** in the presence of CN^-, molecular modeling was performed by using the density function theory with B3LYP using 6-31G(d,p) basis sets implanted in a Gaussian 03 program.[22] The optimized geometries of **1** and **1-CN** are shown in Figure 11. The optimized geometry of sensor 1 was in good agreement with the experimental crystal structures shown in Figure 1. The major chromophore adopts a nearly planar conformation, extending from the 2-cyanoacrylate acceptor to the stilbene moiety. The three aromatic substituents around the N atom maintain an ideal trigonal planar shape ($\theta = 360°$). The ground-state geometry undergoes an apparent twist upon the addition of CN^-, while the π-conjugation between the 2-cyanoacrylate and the stilbene was interrupted. The interruption of the π-conjugation resulted in a substantial blue shift in the absorption spectrum, and decreased the ICT character.

Detailed information about the marked absorption in the blue shift upon nucleophilic cyanide addition with **1** can be obtained from time-dependent DFT (TDDFT) calculations as well. The results of transitions with an oscillator strength above 0.1 are summarized in Table 2. The calculated absorption wavelengths of **1** and **1-CN** were 524 nm and 414 nm, respectively, with oscillator strengths of 1.00 and 1.06. The calculated hypsochromic shift is in good agreement with experimental results. The simulated spectra of **1** and **1-CN** are shown in Figure S10 (See the Supporting Information).

The calculated electron distributions in the frontier molecular orbitals of **1** and **1-CN** are shown in Figure 12. For comparison, the corresponding data for **3** are also included in Figure 12. In the case of **1**, the electron density in the HOMO is localized mainly on the triphenylamine (TPA) moiety, while the LUMO is localized on the 2-cyanoacrylic acid ethyl ester. A charge separation is expected to be produced while an electron is promoted from the HOMO to the LUMO. However, the electron distribution in **1-CN**, particularly in the LUMO, is different from that of **1**. Because of the saturation of a C=C bond, the electron population in the LUMO of **1-CN** is confined on the stilbene moieties, without involving the cyanoacrylate. The electronic configuration of **1-CN** is analogous to that of **3**, as well as their high fluorescence quantum efficiencies.[16] The calculated electronic nature of **1** complies nicely with the experimental observations (Figure 5).

Table 2. Calculated TDDFT excitation energies (E), oscillator strengths (f), MO compositions, and characters for **1** and **1-CN**.

Dye	n[a]	E (ev, nm)	f	Composition	Character
1	1	2.37 (524)	1.00	98% HOMO→LUMO	CT
	2	3.33 (372)	0.99	82% HOMO-1→LUMO	π–π* (1)
	6	3.70 (335)	0.13	93% HOMO→LUMO+3	π–π* (2)
1-CN	1	2.99 (414)	1.06	97% HOMO→LUMO	CT
	5	3.93 (315)	0.16	95% HOMO→LUMO+3	π–π* (1)
	6	3.93 (315)	0.60	93% HOMO-1→LUMO	π–π* (2)

[a] Sequence of calculated transitions in order of energy.

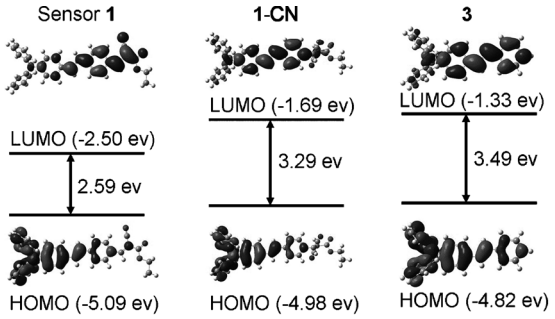

Figure 12. The HOMO and LUMO energy levels and the orbitals of **1**, **1-CN** and **3**.

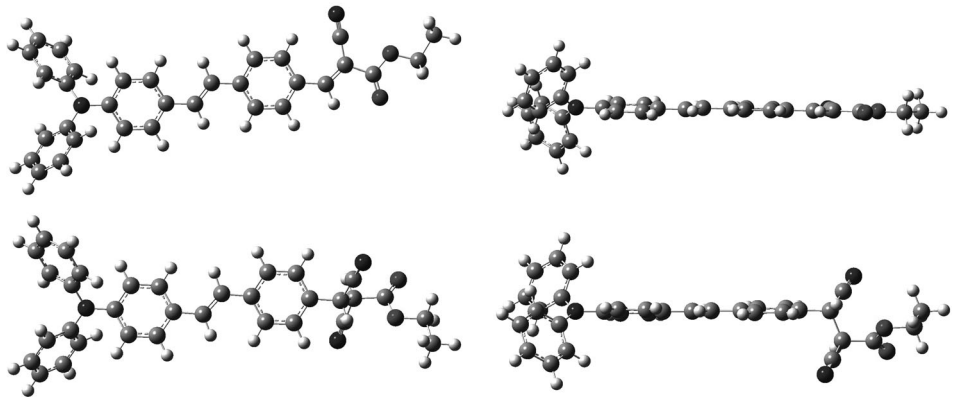

Figure 11. The optimized structures of **1** and **1-CN**$^-$.

Conclusions

A stilbene-based sensor for CN^- in an aqueous THF solution displayed a remarkable selectivity in the presence of other anions. A large blue shift (73 nm) was observed in the absorption spectra in response to CN^-. A ratiometric dual fluorescence was also detected with an intensity enhancement of I_{460}/I_{673} up to 2.25×10^3 fold. The dual fluorescent nature was found to be a result of an

equilibrium between two conformational isomers. This phenomenon can be explained explicitly with the aid of DFT/TDDFT calculations, the spectral blue shift was caused by diminishing the ICT character, therefore inhibiting the fluorescence quenching mechanism.

Experimental Section

General Information

^{1}H and ^{13}C NMR spectra were recorded on a Bruker 400 MHz spectrometer. Fast atom bombardment (FAB) mass spectra were recorded on a Jeol JMS 700 double-focusing spectrometer. UV spectra were measured on a Jasco V-530 double-beam spectrophotometer. Fluorescence spectra were recorded on a Hitachi F-4500 fluorescence spectrophotometer. Absorption and fluorescence sensing measurements were performed in 3×10^{-5} M water/THF (30:70, v/v) solutions in all cases. The aliquots of a freshly prepared anion solution (0.03 M) at defined increments were added to an optical cell containing compound **1** (2 mL) and a magnetic stir bar. Solutions were allowed to equilibrate for 15 min before taking each measurement. Experiments with longer equilibration times did not produce noticeable differences. A nitrogen bubbled solution of anthracene ($\Phi_f=0.27$ *n*-hexane)[23] was used as a standard for the fluorescence quantum yield determinations. An error of 10% is estimated for the fluorescence quantum yields. Fluorescence lifetimes were also measured at room temperature by using a Edinburgh FLS920 spectrometer. The instrument response function was calibrated by a scatter solution using a gated hydrogen arc lamp. The goodness of the nonlinear least-squares fit was judged by the reduced χ^2 value (<1.2 in all cases), the randomness of the residuals, and the autocorrelation function. Solvents of reagent grade were used for syntheses, and those of spectroscopy grade for spectra measurements. Compounds purchased from commercial sources were used as received. The syntheses of compounds **5**[18] and **6**[17] have been reported previously.

Synthesis

*2-Cyano-3-{4-[2-(4-diphenylamino-phenyl)-vinyl]-phenyl}-acrylic acid ethyl ester (**1**)*

An acetic acid solution of **4** (0.5 g, 1.30 mmol), ethyl cyanoacetate (0.2 mL, 13.40 mmol), and ammonium acetate (0.03 g, 0.33 mmol) was stirred at 90 °C for 24 h. The organic layer was separated and dried over $MgSO_4$. After the solvent was removed under reduced pressure, the crude product was recrystallized in CH_2Cl_2/*n*-hexane to afford the desired product **1** (0.40 g, 67%) as an orange solid. M.p. 237–238 °C; ^{1}H NMR (400 MHz, [D$_8$]THF): $\delta=8.24$ (s, 1H), 8.06 (d, $J=8.4$ Hz, 2H), 7.69 (d, $J=8.4$ Hz, 2H), 7.48 (d, $J=8.4$ Hz, 2H), 7.36 (d, $J=16.4$ Hz, 1H), 7.28–7.24 (m, 4H), 7.14 (d, $J=16.4$ Hz, 1H), 7.11 (d, $J=8.4$ Hz, 2H), 7.05–7.01 (m, 5H), 4.32 (q, $J=7.1$ Hz, 2H), 1.35 ppm (t, $J=7.1$ Hz, 3H); ^{13}C NMR (100 MHz, [D$_8$]THF): $\delta=163.35$, 154.36, 149.35, 148.63, 144.16, 132.80, 132.62, 132.03, 131.58, 130.33, 128.98, 127.78, 126.42, 125.79, 124.36, 123.93, 116.40, 102.76, 63.08, 14.60 ppm; FAB-HRMS calcd for $C_{32}H_{27}N_2O_2$ [M+H$^+$] 471.2072, found 471.2079.

*4-[2-(4-Diphenylamino-phenyl)-vinyl]-2,6-dimethyl-benzaldehyde (**7**)*

A heterogeneous mixture of triethylamine (2.1 mL), **5** (1.59 g, 7.46 mmol), $Pd(OAc)_2$ (0.033 g, 2 mol%), P(o-tolyl)$_3$ (0.091 g, 4 mol%), and **6** (2.23 g, 8.2 mmol) under argon were heated at 80 °C for 18 h. The solution was cooled and then CH_2Cl_2 (40 mL) was added. The insoluble residue was filtered off and the filtrate was concentrated in vacuo to afford the crude product. Column chromatograph with ethyl acetate/*n*-hexane (1:20) afforded the desired product as a yellow solid (1.96 g, 65% yield). M.p. 145–146 °C; ^{1}H NMR (400 MHz, $CDCl_3$): $\delta=10.58$ (s, 1H), 7.40 (d, $J=8.5$ Hz, 2H), 7.30–7.26 (m, 4H), 7.20 (s, 2H), 7.15–7.12 (m, 5H), 7.08–7.04 (m, 4H), 6.92 (d, $J=16.2$ Hz, 1H), 2.64 ppm (s, 6H); ^{13}C NMR (100 MHz, $CDCl_3$): $\delta=192.57$, 148.06, 147.36, 142.03, 141.82, 131.16, 131.05, 130.56, 129.33, 127.71, 127.41, 125.42, 124.77, 123.34, 123.05, 20.72 ppm; FAB-HRMS calcd for $C_{29}H_{26}NO$ [M+H$^+$] 404.2014, found 404.2025.

*2-Cyano-3-{4-[2-(4-diphenylamino-phenyl)-vinyl]-2,6-dimethyl-phenyl}-acrylic acid ethyl ester (**2**)*

An acetic acid solution of **7** (0.85 g, 2.1 mmol), ethyl cyanoacetate (2.4 g, 21 mmol), and ammonium acetate (0.04 g, 0.53 mmol) was stirred at 90 °C for 24 h. The organic layer was separated and dried over $MgSO_4$. After the solvent was removed under reduced pressure, the crude product was recrystallized in CH_2Cl_2/MeOH to afford the desired product **2** (0.66 g, 63%) as light-orange solid. M.p. 161–162 °C; ^{1}H NMR (400 MHz, $CDCl_3$): $\delta=8.51$ (s, 1H), 7.39 (d, $J=8.4$ Hz, 2H), 7.29–7.24 (m, 6H), 7.14–7.03 (m, 9H), 6.92 (d, $J=16.0$ Hz, 1H), 4.41 (q, $J=7.1$ Hz, 2H), 1.43 ppm (t, $J=7.1$ Hz, 3H); ^{13}C NMR (100 MHz, $CDCl_3$): $\delta=161.54$, 157.38, 147.72, 147.45, 139.34, 136.71, 130.98, 130.35, 129.71, 129.30, 127.53, 126.01, 125.82, 124.63, 123.29, 123.17, 114.44, 110.60, 62.76, 20.48, 14.11 ppm; FAB-HRMS calcd for $C_{34}H_{31}N_2O_2$ [M+H$^+$] 499.2385, found 499.2398.

Quantum Chemistry Computation

Computations were performed using the Gaussian 03 program package.[22] The geometry was optimized by using B3LYP (Becke three parameters hybrid functional with Lee–Yang–Parr correlation functionals) with the Pople 6–31G(d,p) atomic basis set.[22b,c]

Acknowledgements

Financial support was provided in part by the National Science Council of the Republic of China. We thank Professor J.-S. Yang for the lifetime measurements.

[1] a) P. D. Beer, P. A. Gale, *Angew. Chem.* **2001**, *113*, 502; *Angew. Chem. Int. Ed.* **2001**, *40*, 486; b) V. Amendola, D. Esteban-Gómez, L. Fabbrizzi, M. Licchelli, *Acc. Chem. Res.* **2006**, *39*, 343; c) S. K. Kim, J. H. Bok, R. A. Bartsch, J. Y. Lee, J. S. Kim, *Org. Lett.* **2005**, *7*, 4839; d) H. J. Kim, S. K. Kim, J. Y. Lee, J. S. Kim, *J. Org. Chem.* **2006**, *71*, 6611; e) J. S. Kim, D. T. Quang, *Chem. Rev.* **2007**, *107*, 3780.

[2] a) K. W. Kulig, *Cyanide Toxicity*, U.S. Department of Health and Human Services, Atlanta, GA, **1991**; b) S. I. Baskin, T. G. Brewer, *Medical Aspects of Chemical and Biological Warfare*, (Eds: F. Sidell, E. T. Takafuji, D. R. Franz), TMM Publication, Washington, DC, **1997**, ch. 10, pp. 271–286.

[3] a) C. Young, L. Tidwell, C. Anderson, *Cyanide: Social, Industrial and Economic Aspects*, Minerals, Metals, and Materials Society, Warrendale, **2001**; b) G. C. Miller, C. A. Pritsos, *Cyanide: Soc. Ind. Econ. Aspects, Proc. Symp. Annu. Meet. TMS* **2001**, 73–81.

[4] a) Z. Xu, X. Chen, H. A. Kim, J. Yoon, *Chem. Soc. Rev.* **2010**, *39*, 127; b) P. Anzenbacher, Jr., D. S. Tyson, K. Jursíková, F. N. Castellano, *J. Am. Chem. Soc.* **2002**, *124*, 6232; c) Z. Lin, H. C. Chen, S.-S. Sun, C.-P. Hsu, T. J. Chow, *Tetrahedron* **2009**, *65*, 5216; d) S.-H. Kim, S.-J. Hong, J. Yoo, S.-K. Kim, J. L. Sessler, C.-H. Lee, *Org. Lett.* **2009**, *11*, 3626.

[5] a) V. Ganesh, M. P. C. Sanz, J. C. Mareque-Rivas, *Chem. Commun.* **2007**, 5010; b) Q. Zeng, P. Cai, Z. Li, J. Qina, B. Z. Tang, *Chem. Commun.* **2008**, 1094; c) X. Lou, L. Zhang, J. Qin, Z. Li, *Chem. Commun.* **2008**, 5848; d) J. V. Ros-Lis, R. Martínez-Máñez, J. Soto, *Chem. Commun.* **2005**, 5260; e) T. W. Hudnall, F. P. Gabbaï, *J. Am. Chem. Soc.* **2007**, *129*, 11978; f) A. Touceda-Varela, E. I. Stevenson, J. A. Galve-Gasión, D. T. F. Dryden, J. C. Mareque-Rivas, *Chem. Commun.* **2008**, 1998; g) S.-Y. Chung, S.-W. Nam, J. Lim, S. Park, J. Yoon, *Chem. Commun.* **2009**, 2866.

[6] J. V. Ros-Lis, R. Martínez-Máñez, J. Soto, *Chem. Commun.* **2002**, 2248.

[7] Y.-K. Yang, J. Tae, *Org. Lett.* **2006**, *8*, 5721.

[8] a) M. Tomasulo, F. M. Raymo, *Org. Lett.* **2005**, *7*, 4633; b) M. Tomasulo, S. Sortino, A. J. P. White, F. M. Raymo, *J. Org. Chem.* **2006**, *71*, 744.
[9] Y. M. Chung, B. Raman, D. S. Kim, K. H. Ahn, *Chem. Commun.* **2006**, 186.
[10] a) D.-G. Cho, J. H. Kim, J. L. Sessler, *J. Am. Chem. Soc.* **2008**, *130*, 12163; b) J. L. Sessler, D.-G. Cho, *Org. Lett.* **2008**, *10*, 73.
[11] a) S.-J. Hong, J. Yoo, S.-H. Kim, J. S. Kim, J. Lee, C.-H. Yoon, *Chem. Commun.* **2009**, 189; b) S. Vallejos, P. Estévez, F. C. García, F. Serna, J. L. de La Peña, J. M. García, *Chem. Commun.* **2010**, *46*, 7951; c) Z. Liu, X. Wang, Z. Yang, W. He, *J. Org. Chem.* **2011**, *76*, 10286; d) C.-H. Lee, H.-J. Yoon, J.-S. Shim, W.-D. Jang, *Chem. Eur. J.* **2012**, *18*, 4513; e) Y.-D. Lin, Y.-S. Peng, W. Su, C.-H. Tu, C.-H. Sun, T. J. Chow, *Tetrahedron* **2012**, *68*, 2523.
[12] a) D. T. Quang, J. S. Kim, *Chem. Rev.* **2010**, *110*, 6280; b) A. P. Demchenko, *Introduction to Fluorescence Sensing*, Springer, New York, **2008**.
[13] a) X. Zhang, Y. Xiao, X. Qian, *Angew. Chem.* **2008**, *120*, 8145; *Angew. Chem. Int. Ed.* **2008**, *47*, 8025; b) J. V. Mello, N. S. Finney, *Angew. Chem.* **2001**, *113*, 1584; *Angew. Chem. Int. Ed.* **2001**, *40*, 1536; c) A. Coskun, E. U. Akkaya, *J. Am. Chem. Soc.* **2005**, *127*, 10464; d) R. Y. Tsien, A. T. Harootunian, *Cell Calcium* **1990**, *11*, 93; e) A. P. Demchenko, *J. Fluoresc.* **2010**, *20*, 1099; f) Y. Bao, B. Liu, H. Wang, J. Tian, R. Bai, *Chem. Commun.* **2011**, *47*, 3957.
[14] M. S. Tremblay, M. Halim, D. Sames, *J. Am. Chem. Soc.* **2007**, *129*, 7570.
[15] a) H. Yu, M. Fu, Y. Xiao, *Phys. Chem. Chem. Phys.* **2010**, *12*, 7386; b) X. Lv, J. Liu, Y. Liu, Y. Zhao, M. Chen, P. Wang, W. Guo, *Org. Biomol. Chem.* **2011**, *9*, 4954; c) G. Qian, X. Li, Z. Y. Wang, *J. Mater. Chem.* **2009**, *19*, 522; d) C.-L. Chen, Y.-H. Chen, C.-Y. Chen, S.-S. Sun, *Org. Lett.* **2006**, *8*, 5053; e) H. Yu, Q. Zhao, Z. Jiang, J. Qin, Z. Li, *Sens. Actuators B* **2010**, *148*, 110; f) L. Yuan, W. Lin, Y. Yang, J. Song, J. Wang, *Org. Lett.* **2011**, *13*, 3730; g) X. Lv, J. Liu, Y. Liu, Y. Zhao, Y.-Q. Sun, P. Wang, W. Guo, *Chem. Commun.* **2011**, *47*, 12843.
[16] a) J.-S. Yang, ; Y.-D. Lin, Y.-H. Chang, S.-S. Wang, *J. Org. Chem.* **2005**, *70*, 6066; Y.-D. Lin, Y.-H. Lin, F.-L. Liao, *J. Org. Chem.* **2004**, *69*, 3517 S.-Y. Chiou, K.-L. Liau, *J. Am. Chem. Soc.* **2002**, *124*, 2518; b) C.-K. Lin, C. Prabhakar, J.-S. Yang, *J. Phys. Chem. A* **2011**, *115*, 3233.
[17] a) S. Hwang, J. H. Lee, C. Park, H. Lee, C. Kim, C. Park, M.-Y. Lee, W. Lee, J. Park, K. Kim, N. G. Park, C. Kim, *Chem. Commun.* **2007**, 4887; b) Y.-D. Lin, T. J. Chow, *J. Mater. Chem.* **2011**, *21*, 14907; c) Y.-D. Lin, T. J. Chow, *J. Photochem. Photobiol. A* **2012**, *230*, 47; d) Y.-D. Lin, C.-T. Chien, S.-Y. Lin, H.-H. Chang, C.-Y. Liu, T. J. Chow, *J. Photochem. Photobiol. A* **2011**, *222*, 192.
[18] R. J. Kumar, S. Karlsson, D. Streich, A. R. Jensen, M. Jäger, H.-C. Becker, J. Bergquist, O. Johansson, L. Hammarström, *Chem. Eur. J.* **2010**, *16*, 2830.
[19] CCDC 885863 contains the supplementary crystallographic data for this paper. These data can be obtained free of charge from The Cambridge Crystallographic Data Centre at www.ccdc.cam.ac.uk/data_request/cif.
[20] a) J.-S. Yang, ; Y.-D. Lin, Y.-H. Lin, F.-L. Liao, *J. Org. Chem.* **2004**, *69*, 3517; b) J.-S. Yang, ; Y.-D. Lin, Y.-H. Chang, S.-S. Wang, *J. Org. Chem.* **2005**, *70*, 6066.
[21] a) A. N. Fletcher, *J. Phys. Chem.* **1968**, *72*, 2742; <lit *b*> O. S. Khalil, C. J. Selinskar, S. P. McGlynn, *J. Chem. Phys.* **1973**, *58*, 1607; c) K.-I. Itoh, T. Azumi, *J. Chem. Phys.* **1975**, *62*, 3431; d) J. R. Lakowich, *Principles of Fluorescence Spectroscopy*, Academic/Plenum Publishing, New York, **1999**, pp. 194–448.
[22] a) Gaussian 03, M. J. Frisch, G. W. Trucks, H. B. Schlegel, G. E. Scuseria,M. A. Robb, J. R. Cheeseman, J. A. Montgomery, Jr, T. Vreven,K. N. Kudin, J. C. Burant, J. M. Millam, S. S. Iyengar, J. Tomasi,V. Barone, B. Mennucci, M. Cossi, G. Scalmani, N. Rega,G. A. Petersson, H. Nakatsuji, M. Hada, M. Ehara, K. Toyota,R. Fukuda, J. Hasegawa, M. Ishida, T. Nakajima, Y. Honda,O. Kitao, H. Nakai, M. Klene, X. Li, J. E. Knox, H. P. Hratchian,J. B. Cross, C. Adamo, J. Jaramillo, R. Gomperts,R. E. Stratmann, O. Yazyev, A. J. Austin, R. Cammi, C. Pomelli,J. W. Ochterski, P. Y. Ayala, K. Morokuma, G. A. Voth,P. Salvador, J. J. Dannenberg, V. G. Zakrzewski, S. Dapprich,A. D. Daniels, M. C. Strain, O. Farkas, D. K. Malick,A. D. Rabuck, K. Raghavachari, J. B. Foresman, J. V. Ortiz,Q. Cui, A. G. Baboul, S. Clifford, J. Cioslowski, B. B. Stefanov,G. Liu, A. Liashenko, P. Piskorz, I. Komaromi, R. L. Martin,D. J. Fox, T. Keith, M. A. Al-Laham, C. Y. Peng, A. Nanayakkara, M. Challacombe, P. M. W. Gill, B. Johnson,W. Chen, M. W. Wong, C. Gonzalez, J. A. Pople, Gaussian Inc., Pittsburgh, PA, **2003**; b) C. Lee, W. Yang, R. G. Parr, *Phys. Rev. B* **1988**, *37*, 785; c) A. D. Becke, *J. Chem. Phys.* **1993**, *98*, 5648.
[23] W. R. Dawson, M. W. Windsor, *J. Phys. Chem.* **1968**, *72*, 3251.

Received: June 28, 2012
Published online: ■■ ■■, 0000

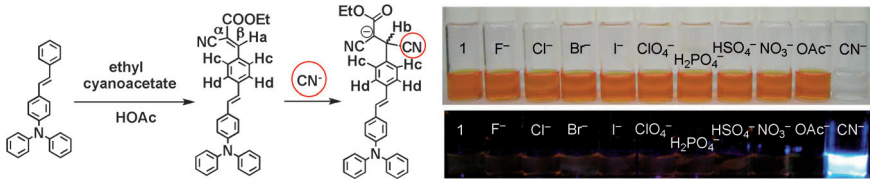

Sense and sensitivity: A highly efficient and selective colorimetric and ratiometric fluorescent sensor for detection of cyanide in aqueous media has been developed. This sensor exhibits a distinctive color change upon reaction with cyanide, along with significant fluorescence amplification. The sensing mechanism is discussed with the aid of spectral analyses and DFT/TDDFT calculations.

Fluorescent Sensors

*Yan-Duo Lin, Yung-Shu Pen, Weiting Su, Kang-Ling Liau, Yun-Sheng Wen, Chin-Hsin Tu, Chia-Hsing Sun, Tahsin J. Chow** ____ ▮▮▮▮–▮▮▮▮

Reaction-Based Colorimetric and Ratiometric Fluorescence Sensor for Detection of Cyanide in Aqueous Media

